



DesaLink: solar powered desalination of brackish groundwater giving high output and high recovery

T.Y. Qiu, O.N. Igobo, P.A. Davies*

Sustainable Environment Research Group, School of Engineering and Applied Science, Aston University, Birmingham B4 7ET, UK

Tel. +44 0 121 204 3724; Fax: +44 0 121 204 3683; email: p.a.davies@aston.ac.uk

Received 27 February 2012; Accepted 18 July 2012

ABSTRACT

Desalination of groundwater is essential in many arid areas that are far from both seawater and fresh water resources. The ideal groundwater desalination system should operate using a sustainable energy source and provide high water output per land area and cost. To avoid discharging voluminous brine, it should also provide high recovery. To achieve these aims, we have designed DesaLink, a novel approach to linking the solar Rankine cycle to reverse osmosis (RO). To achieve high recovery without the need for multiple RO stages, DesaLink adopts a batch mode of operation. It is suited to use with a variety of solar thermal collectors including linear Fresnel reflectors (LFR). For example, using a LFR occupying 1,000 m² of land and providing steam at 200°C and 15.5 bar, DesaLink is predicted to provide 350 m³ of fresh water per day at a recovery ratio of 0.7, when fed with brackish groundwater containing 5,000 ppm of sodium chloride. Here, we report preliminary experiments to assess the feasibility of the concept. We study the effects of longitudinal dispersion, concentration polarisation and describe a pilot experiment to demonstrate the batch process using a materials testing machine. In addition, we demonstrate a prototype of DesaLink running from compressed air to simulate steam.

Keywords: Reverse osmosis; Solar; Brackish water; Groundwater; Batch mode; DesaLink

1. Introduction

Water scarcity, as one of the most concerned global challenges, as illustrated in Fig. 1, is complicated by population growth, industrialisation and climate change. Alongside existing water conservation remedies, desalination by thermal or membrane means can be a more proactive and dynamic way to water this thirsty world on our “blue planet”. Since 1980s, the vast majority of desalination plants have implemented reverse osmosis (RO) instead of thermal tech-

nology, thanks to its much lower-energy consumption. Nowadays large-scale seawater RO systems consume much less energy—in the past, to produce 1 m³ of water from seawater, some 10–15 kilowatt-hours (kWh) was required comparing to 2–3 kWh/m³ today. However, most of the current RO systems are still proving to be too energy intensive when it comes to desalination of brackish groundwater at small scale, due to relatively smaller components and lack of using energy recovery devices [1]. Desalination of groundwater is essentially and even urgently needed in many arid areas having

*Corresponding author.

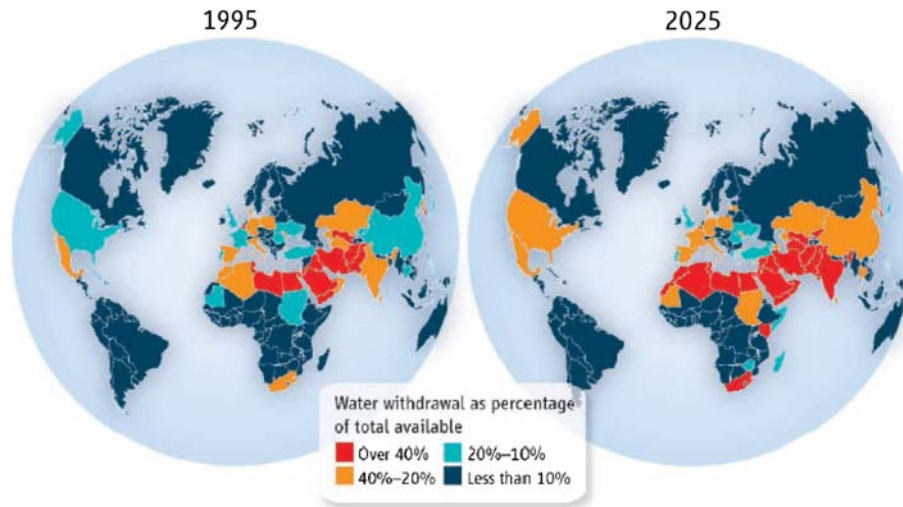


Fig. 1. Spreading water shortages—presently, 1 billion people do not have access to clean water, 2.3 billion people live in water-stressed areas and this number expected to climb to 3.5 billion by 2025, from Ref. [11].

adequate groundwater resources but which are far from both seawater and fresh water resources, like some arid parts of India, China and the USA. To be competitive, a brackish groundwater RO (BWRO) system should operate economically—provide high water output per land area and low-energy consumption. This not only relies on the components, e. g. low-energy RO membrane, high efficiency pump, but also depends on the excellent system design.

Another major challenge of inland BWRO desalination is brine disposal. Khan et al. [2] have given a comprehensive review about brine management in which several methods of brine disposal are described and compared, all these methods raise technical and economical concerns, more importantly, the elevated salinity of BWRO brines (more than twice that of brackish groundwater) poses environmental risks [2,3]. Thus, an ideal BWRO desalination system should recover as much brackish water as possible, i.e. minimise brine volume and maximise system productivity. However, high recovery ratio usually implies large energy inputs. Additionally, with respect to high cost and environmentally unfriendly nature of fossil fuel, BWRO systems should be powered by some sustainable energy sources, e.g. solar energy, and this versatility could make them especially advantageous for developing countries.

To achieve these aims, we have designed DesaLink, a novel approach to linking the solar Rankine cycle (RC) to a batch mode RO [4]. The batch RO can be contrasted with the conventional continuous flow RO operation in which concentration increases significantly from the inlet to the outlet of the RO module.

This longitudinal concentration gradient increases the energy requirement especially at high recovery ratios. One possible approach to minimise this effect is to provide several RO stages in series, with intermediate pumps in place to supply appropriate pressure to each stage [1,5]. This staged membrane operation allows certain volumes of water to be brought to the corresponding higher pressures, thereby diminishing the longitudinal concentration gradient-related energy loss. With an infinite number of stages, the energy usage would approach the theoretical minimum; however, this design is impractical and the saved energy may not offset the additional capital cost.

In the batch RO process, concentration is kept almost uniform through the system at each moment in time and wastage of energy due to concentration gradients inside the system is therefore minimised [4]. In principle, the specific energy consumption (SEC) of a batch system can approach the ideal value. Moreover, the batch system is of particular interest for direct coupling with the solar powered RC. To date, though several design studies [6–8] have indicated that the performance of such Rankine-RO systems should be comparable with those of photovoltaic-RO systems, practical experience has shown rather lower efficiencies [9,10]. The DesaLink is expected to give significant improvements by only adopting linkages to couple solar RC and batch RO, because all unnecessary energy conversion steps are eliminated.

In this paper, we introduce the design of DesaLink and assess the energy efficiency of batch RO system with highlighting the solutions to the negative factors: (i) the longitudinal dispersion and (ii) the

concentration polarisation (CP). We also describe a pilot experiment to demonstrate the batch process using a materials testing machine. We compare these results to model predictions obtained earlier before moving onto elucidate how the concept will be developed further.

2. DesaLink development

The feasibility of photovoltaic RO for brackish groundwater desalination at remote sites has been proven. It is a simple standalone system indeed. But the main drawbacks of the solar cell technology are the high cost and low efficiency. Another novel desalination combination which is solar RC driven RO technology is also on the horizon. It is still at the early stage of research and development, the knowledge and experience on solar RC-RO desalination is very scarce [1]. A principal drawback in using the steam RC at small scales is that the steam turbines typically used tend to become unattractive at the low power outputs due to the blade friction losses and leakage losses in the turbine. Instead of using a turbine to convert the linear motion of the steam power piston to rotary motion, an alternative is to use a piston to expand the steam. A so-called steam pump may be used meaning that its piston is directly coupled to that of a reciprocating pump. However, a shortcoming with steam pumps is that the force provided by the power piston varies as the piston moves over its cycle. The DesaLink solves this problem by mechanical means which overcomes the varying forces. Another advantage of the DesaLink is the ability to drive directly from a steam piston a batch RO process, which is in principle with the most energy efficient way of operating RO and therefore increases the water output.

2.1. The batch RO process

Fig. 2 illustrates the operation of the batch RO system which consists of three principle stages. To overcome the typical lack of energy recovery devices in conventional BWRO system, this cyclic mode operation process obviates the need for costly energy recovery devices by recirculating the pressurised feed.

2.2. A wise choice of crank mechanism

The principal concept of DesaLink is shown in Fig. 3. Notably, the force available from the power piston decreases while the force required to pressurise the pump piston increases. By using a simple arrangement 'consisting of a crank (OP) and linkages (LP and

MP) to couple the two pistons, an increasing mechanical advantage will be obtained as the pistons move. In the previous work of Davies [4], the crank mechanism was analysed in detail and its efficiency was assessed to be in the range of 55–94% according to the expansion ratio of steam, recovery ratio, etc. In order to recover more groundwater without compromising the efficiency, 70% recovery ratio was chosen, thus the volume of the pump cylinder was determined. Based on work balance between the energy generated by steam expansion and the needed separation energy, the volume of feed steam and the volume of the power cylinder were also obtained [4]. The system parameters are given in Table 1 (the RO membrane element is Dow FILMTEC™ type BW30-2540).

By applying simple trigonometry and work balance, the displacements of the two pistons and the motion of the crank point P can be calculated along the whole operation process. The comparison to the ideal movement relationship between the two pistons is illustrated in Fig. 4. In addition, based on the polytropic expression which describes steam expansion and the van't Hoff equation, the variation of the pressures in the two cylinders is shown in Fig. 5, together with the achieved mechanical advantage.

Based on the foregoing analysis, the DesaLink pressurisation cycle will take seven minutes and it is capable to produce three litres fresh water per cycle, and thus, 75% recovery ratio is achieved. Assuming the DesaLink power cylinder is powered by 1,000 m² area of linear Fresnel reflectors (LFRs) with 35% collection efficiency, which is providing steam at 200°C and 15.5 bar, DesaLink is predicted to provide 350 m³ of fresh water per day at a recovery ratio of 0.7, when fed with brackish groundwater containing 5,000 ppm of sodium chloride [4].

3. Preliminary experiments

3.1. The batch-mode test

The batch mode RO tests were performed prior to building the whole DesaLink. The tests were intended to investigate the applicability of mechanically driven BWRO desalination system by evaluating the fresh water production against the mechanically provided pressures. Other design factors, including the sealing piston arrangement, sealing of pump piston, etc., were also examined in these tests. The batch mode RO system (depicted in Fig. 2) was set up as illustrated in Fig. 6. The experiments were conducted with the use of a materials testing (Instron®) machine, which is able to provide desired, varying pressurising forces in order to maintain a constant displacement rate. Before the start

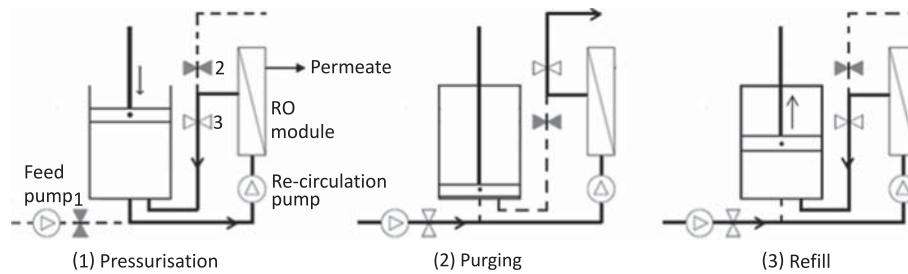


Fig. 2. Initially, both the pump cylinder and RO module are filled with saline water, (1) pressurisation stage (with valve 3 open, valves 1 and 2 closed) the piston pressurises the water, causing fresh water to pass through the membrane. The concentration of solution increases gradually. The concentrations at the inlet and the outlet of the module are kept nearly equal with the help of the re-circulation pump. After the pump piston reaches the end of the cylinder, only concentrated brine is left in the module. So it is necessary to purge the module by introducing feed water (with valves 1 and 2 open, valve 3 closed). In the purging stage, the concentration at the outlet decreases towards the value at the inlet. After washing out the left concentrate, the feed pump feeds saline water into the cylinder to move the piston upwards (with valves 1 and 3 open while valve 2 is closed); thus, the whole system is refilled and restored to its ready-to-go state. The water flow paths and no-flow paths of all the pipes are shown by bold and dashed lines, respectively [6].

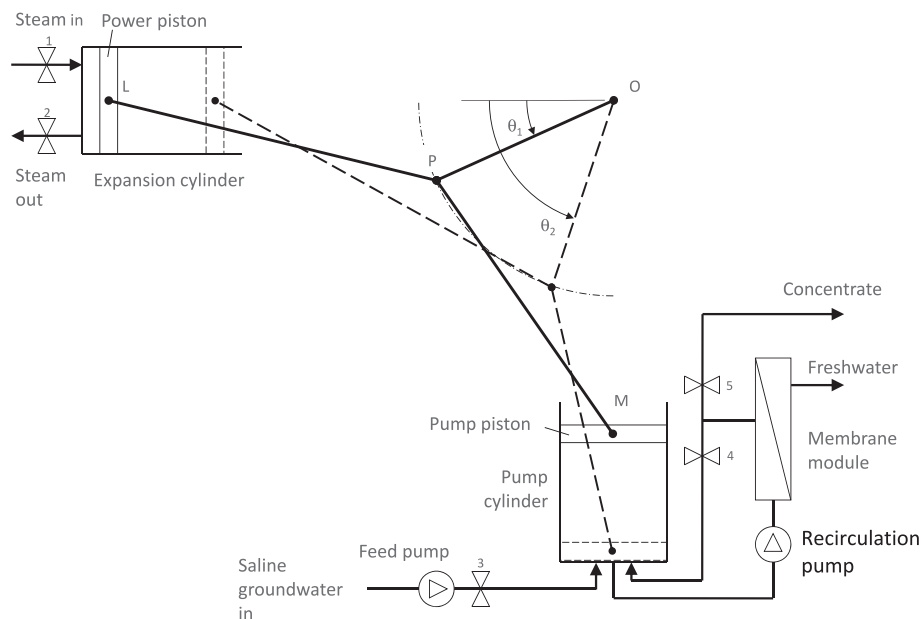


Fig. 3. In this arrangement, the power piston drives the pump piston via a crank mechanism in which the crank OP rotates about the fixed point O. The initial and final positions of the system are shown in bold and dashed lines, respectively, from Ref. [4].

of each test, both the pump cylinder and the RO module were filled with 3,500 ppm sodium chloride (NaCl) solution. In addition, by utilizing the re-circulating pump and vibrating the RO module manually, any trapped air in the whole system cycle was eliminated. Then, the Instron machine was set at a constant displacement rate to compress the pump piston against the solution. Flow pressures and permeate rates were recorded along the process. Once the pump piston reached its end, the Instron machine was stopped. Subsequently, a chart with loading vs. piston displacement

was generated. Notably, the tests were conducted to evaluate only the pressurisation stage of the batch mode operation, because of the limitation of the laboratory environment.

To simulate the predicted movement of the pump piston in Section 2.1, a compressive rate of 50 mm/min was adopted initially. After calibrating the force and the displacement to zero, the Instron machine was started, forcing the piston of pump cylinder to move downwards. The compressive load increased as shown in Fig. 7 and the applied pressure increased

Table 1
The system parameters

	Power piston	Pump piston
Crank radius	0.25 m	0.35 m
Offset of cylinder axis from crank pivot	−0.28 m	−0.2 m
Length of connecting linkage	0.76 m	0.5 m
Initial angular position	0°	45°
Final angular position	55°	100°
Initial piston position from cylinder end	0 m	0 m
Piston area	0.035 m ²	0.0086 m ²
Initial pressure (abs)	9 bar	3.12 bar
Index of polytropic expansion	1.1	–
Angular displacement	55°	–
Stroke length	0.228 m	0.35 m
Cylinder volume	0.008m ³	0.0031m ³
Feed concentration	–	4,000 ppm
<i>RO membrane module (Dow FILMTEC™ type BW30-2540)</i>		
RO module volume	0.001m ³	
Membrane Permeability	1.00E-11 m/sPa	
Membrane salt transfer coefficient	1.80E-07 m/s	
Membrane area	2.6m ²	
Feed channel height	0.071 cm	

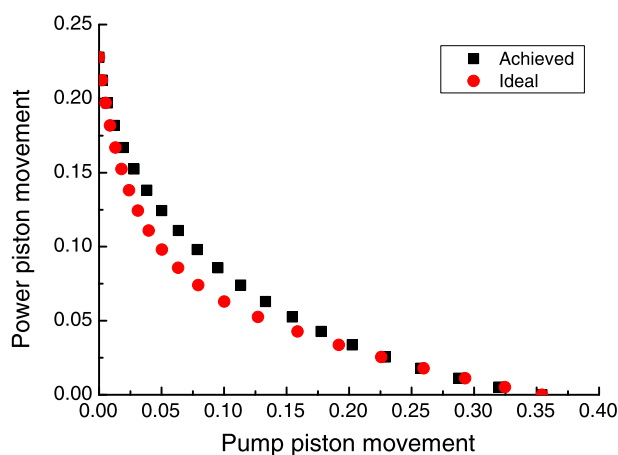


Fig. 4. Actual vs. ideal motion based on work balance (dimensionless variables used).

correspondingly. At the beginning (O–A), the load was increased linearly until around 4.3 kN (point A). This is due to the build-up of pressure in the solution since below the osmotic pressure no water can pass through the membrane and the volume of the solution remains the same. At point A, the applied pressure reached 4 bar, which just exceeds the osmotic pressure of 3,500 ppm NaCl solution, i.e. 2.8 bar. The fresh water (at around 3 ml/s) was pushed across the membrane by the driving forces provided by the pressure

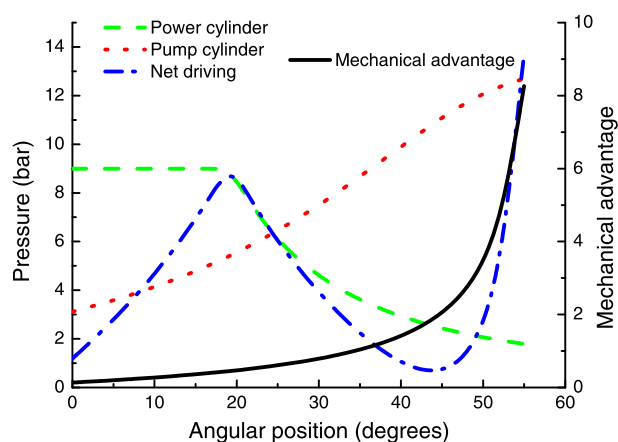


Fig. 5. The crank mechanical advantage enables a remarkable net driving pressure.

difference. With consumption of the compressive energy and reduction of the total solution volume, the pressure increments were reduced (A–B). However, the permeate rate was raised up to 20 ml/s due to the magnified net driving pressure. When the piston reached its end, the maximum pressurising force amounted to 6.5 kN, and the corresponding feed pressure was 11 bar. Permeate was continuously driven out as the pressure gradually decreased to around four bar, eventually achieving equilibrium with the

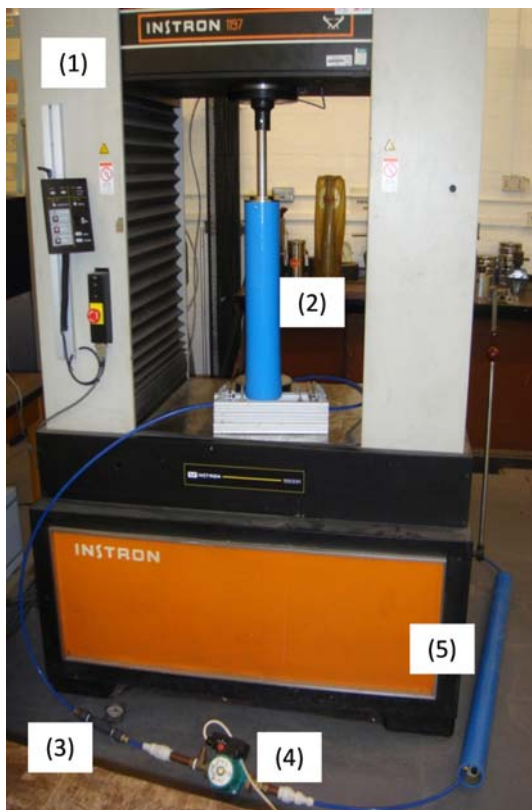


Fig. 6. Batch mode RO test set-up, (1) Material testing (Instron®) machine; (2) Pump cylinder (piston area of 0.0,086 m², length of 0.35 m); (3) Pressure gauge; (4) Re-circulating pump (Wilo, 3 m³/h maximum flow volume) and (5) RO module (Dow FILMTEC™ type BW30-2540). The flow rates of permeate were measured with a stopwatch and measuring cylinders.

osmotic pressure. The total collected permeate was 1,800 ml, i.e. 66% recovery ratio was achieved, and its salinity was under 500 ppm as expected. Notably, these experimental results are in excellent agreement with the proposed performance of batch RO system in Section 2.1; thus, we could confidently argue that the mechanically driven batch RO should be deemed applicable for desalination.

The experiments were also carried out for the following situations: (1) without re-circulating pump and (2) under different compressive displacement rates. Case (1), not surprisingly, underperforms its counterpart with a re-circulating pump and the reasons for this are twofold. Firstly, the trapped air, which could not be eliminated thoroughly, diminished the process performance due to the amount of work wasted on compressing the air rather than the solution (prolonged O–A phase). Secondly, because of the imperfect mixing of the solution and the enhance CP phenomena arose from the absence of rapid

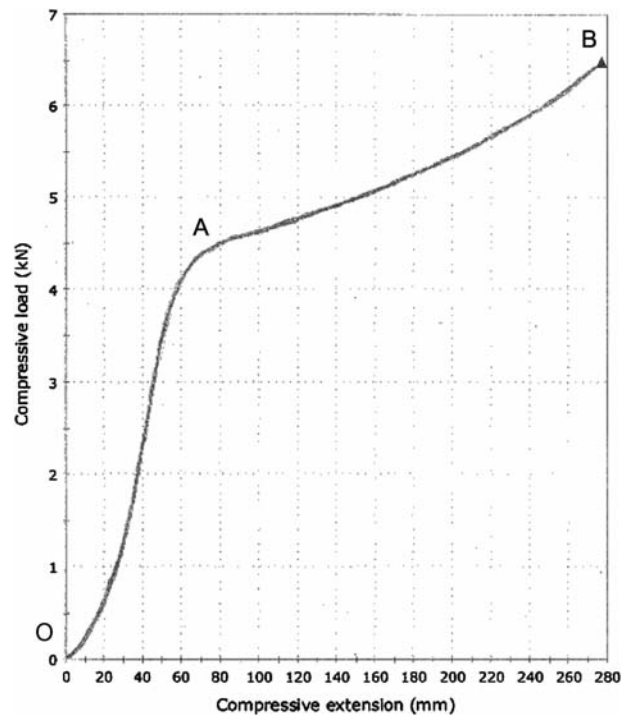


Fig. 7. Result of experiment with re-circulating pump: compressive displacement vs. applied load (proportional to pressure).

circulation flow, the required compressive load was raised by almost 50% (up to 12.5 kN). Case (2) was carried out to investigate the effect of compressive speed on the system performance, therefore allowing us to identify the optimal operation condition. The experiments demonstrated how susceptible the load and pressure are to the chosen compressive displacement rate. On the one hand, a fast compression, e.g. 150 mm/min, would not give adequate time for permeate to cross the membrane and the pressure rose too rapidly, ending up with a huge pressure of 15 bar which could not be provided from the expansion of nine bar compressed air. On the other hand, a slow compressive rate, e.g. 30 mm/min, resulted in a smaller required load (5.74 kN) and pressure (7.5 bar), only 1,000 ml permeate with concentration higher than 500 ppm was obtained which was not desirable.

For the purging phase, ideally, the concentration of the solution at the outlet of the RO module should suddenly drop to the same value as at the input. However, dispersion causes undesirable mixing of the concentrated brine left in the RO module with less concentrated feedwater. Therefore, the salt concentration and energy usage will increase in the following pressurisation cycle. Beside dispersion, the intrinsic CP phenomenon which happens during pressurisation

phase also diminishes DesaLink performance. Therefore, substantial research about dispersion and CP has been conducted to optimise DesaLink.

3.2. Dispersion related energy loss

Undoubtedly, in purging phase, excess of purging water could be applied to bring down the outlet concentration, but this would be an unnecessary waste of feedwater and decrease the recovery ratio of the whole operation. To maintain a continuous operation and achieve high recovery and efficiency, the relationship between the recovery ratio, energy consumption and dispersion should be understood.

By conducting the dispersion research [12], we (i) developed a theory to represent dispersion in spiral wound RO modules and its effect on batch-RO operations; (ii) verified the theory and characterised through experiments the dispersion in specific spiral wound RO modules typically used for brackish water desalination and (iii) as a consequence, quantified the increase in SEC that longitudinal dispersion will cause in practice. The main observations and conclusions on the improvements of DesaLink were drawn and summarised here: the optimum purge volume is equal to the volume of the solution inside the module, i.e. 0.001 m^3 . To reduce operation time and increase productivity, fast flow rates (20–40 ml/s) are likely to be beneficial in practice. In this case, the use of the optimum purge volume will result in deterioration in energy efficiency, relative to the ideal case of zero dispersion, in the range 4.0–5.5% for a recovery ratio in the range 0.5–0.7 (for BW30-2540 and XLE-2540 membrane elements, respectively). This means that the batch RO system should be able to achieve high recovery ratio and thus small reject brine volume with only a minor penalty in energy efficiency.

3.3. Specific CP model

In any membrane separation process, the flux of water through the membrane results in a build-up of salts near the membrane surface; therefore, the salt concentration near the surface of the membrane exceeds that in the bulk of the solution by a factor CP. This transverse gradient of concentration across the channel enclosed by the membranes is referred to as CP. CP is an undesirable phenomenon as it can cause many negative effects on the membrane separation process [13,14], such as decreases osmotic pressure difference and thereby diminishes permeate fluxes, increases salinity of the product water, in addition, leads to membrane fouling and decreased membrane lifetime.

To minimise effectively CP-related energy losses, and to increase the DesaLink efficiency, an approach of varying hydraulic conditions was adopted. By use of a re-circulating pump (see Fig. 6), the rapid circulating flow increases flow velocity and sweeps away salts accumulating near the surface of the membrane. Note that the energy needed to drive the recirculation pump is small compared to the energy needed for the whole system, because it is working against a low pressure corresponding to the hydraulic resistance to cross flow, which is small compared to the osmotic pressure of the fluid. In order to evaluate the contribution of the re-circulation pump in diminishing CP and quantify CP-related energy loss in DesaLink operation, we researched and selected an appropriate mass transport model, and built the specific CP model via experiments.

3.3.1. Transport mechanisms

Several theoretical models of mass transport mechanisms in membrane separation [15,16] were established by analysis of the concentration boundary layer at the membrane surface. The thickness of this boundary layer is established at the equilibrium of three fluxes—as shown in Fig. 8—the salt convective flux, the salt flux through the membrane J_s and the salt back diffusive flux. The analyses of proposed models usually involve solution of the diffusion–convection differential equations with appropriate boundary conditions and simplifying assumptions. Among these

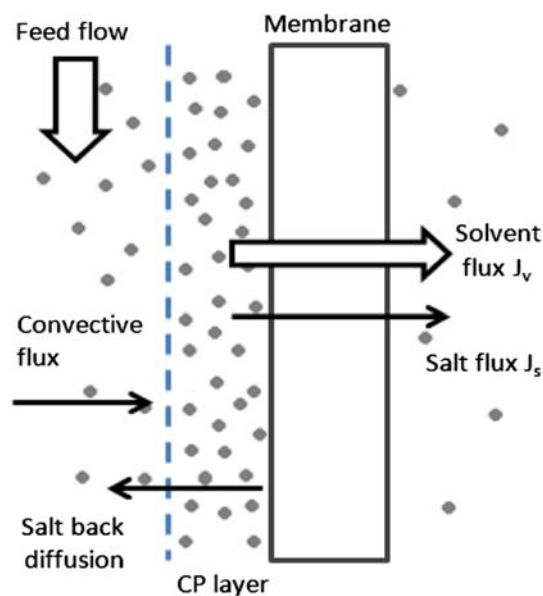


Fig. 8. A detailed representation of membrane separation process.

models, “Film model” is one of the most fundamental theories, and most of the other models were developed based on it.

The simple film model assumes a one-dimensional flow and a fully developed boundary layer. A solute mass balance on a differential fluid element of the boundary layer, equating convective flow towards the membrane surface with the back-diffusion flow, gives the following differential equation:

$$J_s = C_p \cdot J_v = C \cdot J_v - D \cdot \frac{dC}{dy} \quad (1)$$

where J_s is the net solute flux through the membrane, C_p is the permeate solute concentration, J_v is the permeate flux, C is the solute concentration in the boundary layer at a distance y from the membrane surface and D is the solute diffusion coefficient in solvent. Solution of this equation for a boundary layer of thickness δ gives:

$$CP = \frac{C_m - C_p}{C_b - C_p} = \exp\left(\frac{J_v}{k}\right) \quad (2)$$

where k is the mass transfer coefficient and defined as:

$$k = \frac{D}{\delta} \quad (3)$$

The real salt rejection fraction R is:

$$R = \frac{C_m - C_p}{C_m} \quad (4)$$

The observed rejection fraction is given by:

$$R_o = \frac{C_b - C_p}{C_b} \quad (5)$$

Using rejection fractions instead of concentrations, Eq. (2) will become:

$$\frac{1 - R_o}{R_o} = \frac{1 - R_o}{R} \cdot \exp\left(\frac{J_v}{k}\right) \quad (6)$$

Besides the classic film model, there are other models which were derived concerning on various mass transport mechanisms. Sablani et al. [16] reviewed some most popular elementary transport mechanisms proposed from the 1970s onwards. In one, called Kimura–Sourirajan (KS) model (Combined solution–diffusion/film model), this model assumes diffusion is the only mechanism of salt transport in

membrane separation. Solute transport according to this simple solution–diffusion model is given by:

$$J_v = A \cdot (\Delta P - \Delta \pi) \quad (7a)$$

$$J_s = C_p \cdot J_v = P_s \cdot (C_m - C_p) \quad (7b)$$

where J_v is the solvent flux, A is the pure water permeability coefficient, ΔP is the operating pressure and $\Delta \pi$ is the difference in the osmotic pressure across the membrane, which equals $(\pi_m - \pi_p)$. P_s is the salt permeability coefficient.

Combining Eqs. (4), (6) and (7b), and rearranging to eliminate the unknown parameters C_m and R yielding:

$$\frac{C_p}{C_b - C_p} = \frac{1 - R_o}{R_o} = \frac{P_s}{J_v} \cdot \exp\left(\frac{J_v}{k}\right) \quad (8)$$

In our research, we applied the KS model to build the specific CP model for DesaLink.

3.3.2. Determination of mass transfer coefficient k

Generalised correlations of the mass transfer coefficient in fully developed flow follow the Sherwood correlation [17–19]:

$$Sh = \frac{k \cdot d}{D} = a \cdot \left(\frac{du}{v}\right)^\alpha \cdot \left(\frac{v}{D}\right)^\beta = a \cdot Re^\alpha \cdot Sc^\beta \quad (9)$$

where Sh is the Sherwood number, Re is the Reynolds number, Sc is the Schmidt number, d is the hydraulic diameter, u is the flow velocity, v is the kinematic viscosity and a is a numerical constant characterising the flow channel conditions. α and β are empirical constants.

From Eq. (9),

$$K = \frac{u^\alpha}{b} \quad (10)$$

According to the KS and film model, both feed velocity variation and solvent flux variation experimental methods can be adopted to determine the values for k . Despite the applicability of the empirical expressions in form of Eq. (9), using the experimental methods to determine the unknown coefficient in Eq. (9) requires a very wide range of operation pressures to obtain enough quality data points for fitting. This is not practical in this work because of the current limitations of the laboratory equipment. Nevertheless, the quality and robustness of our developed model were

not compromised due to the lack of data points, since a more straightforward experimental procedure was used as follows.

Based on Eq. (7a), for pure water,

$$(J_v)_{\text{water}} = L_p \cdot \Delta P \quad (11)$$

For salt solution,

$$(J_v) = L_p[\Delta P - (\pi_m - \pi_m)] \quad (12)$$

Initially experiments were conducted with pure water (desalinated tap water with concentration of 32 ppm) to determine the membrane (Dow FILM-TEC™ type BW30-2540) permeability L_p , which was 8.44×10^{-12} m/sPa. Note that, this membrane element is around three years old, thus it is understandable why the measured L_p is much lower than the previously provided value of DOW® FilmTec™ [20], 1.00×10^{-11} m/sPa. Then, a series of experiments, with/without the re-circulating pump, in the conventional BWRO desalination operation mode were conducted. In order to determine the relationship between the feed flow rate and the mass transport coefficient k , the feeding pressure was fixed at 3 bar, while various flow rates of the feed solution (780 ppm NaCl), from 2 to 7 cm/s, were adopted. After 1 h, equilibration time for each run, the flow rates and the concentrations of both solvent and solute fluxes were recorded. From Eq. (12), π_m were derived based on measured parameters. We then obtained the CP factors using Eq. (2), and the results indicated that CP factor was reduced by 10% by utilizing the re-circulating pump.

Since the osmotic pressure is proportional to the solution concentration, mass transfer coefficients k at the different feed flow rates u were calculated from Eq. (2). As shown in Fig. 9, k was improved by 50% on average with the help of re-circulating pump. By non-linear fitting of k and u of Eq. (9), a , α and β were determined. The resulting Sherwood correlations specific for our experimental conditions were obtained:

with re – circulating pump:

$$\text{Sh} = 0.08 \cdot \text{Re}^{0.42} \cdot \text{Sc}^{0.41} \quad (13a)$$

without re – circulating pump:

$$\text{Sh} = 0.09 \cdot \text{Re}^{0.37} \cdot \text{Sc}^{0.32} \quad (13b)$$

Assuming the spiral wound membrane element is a rolled-up of two membrane sheets with a channel height d of 0.071 cm, in the feed flow velocity ranging from 1 to 7 cm/s, the Re numbers were smaller than

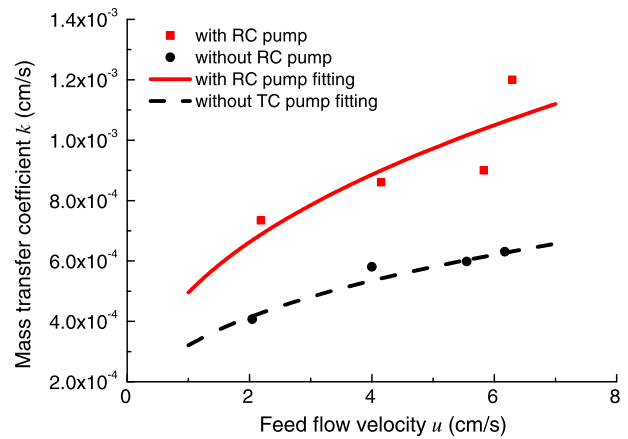


Fig. 9. Mass transfer coefficient k increases with feed flow velocity u .

50. This suggests that our Sherwood correlations can be compared with the empirical Sherwood correlation in a fully developed laminar flow [21] in a smooth channel, which as follow:

$$\text{Sh} = 0.02 \cdot \text{Re}^{0.33} \cdot \text{Sc}^{0.33} \quad (14)$$

The values of α and β , for both the empirical and our correlation, are similar; however, the difference in the parameter a is significant. This can be explained by the different geometrical features of the two models used to derive the correlations. When the solution flows in RO membrane feed channels, unlike in a channel with smooth walls, the value of a is susceptible to flow channel geometry, e.g. radius of curvature, and it is also influenced by the porosity and roughness of the membranes. Therefore, the value of a in the simplified empirical model cannot be considered as the benchmark for our Sherwood correlation. The specifically derived correlation expression for our experimental conditions, as shown in Eq. (13a), is deemed more appropriate and reliable to be used to quantify the CP-related energy losses of DesaLink. Nevertheless, further research is being carried out, and the application of other types of membrane elements is believed to assist in the determination of more accurate correlation parameters.

4. Preliminary result of DesaLink

The first complete prototype of DesaLink has been developed. The experimental work with this prototype provides a step forward beyond the theoretical evaluation under ideal conditions, where the system was analysed without taking into account any energy losses. As mentioned above, the key components of

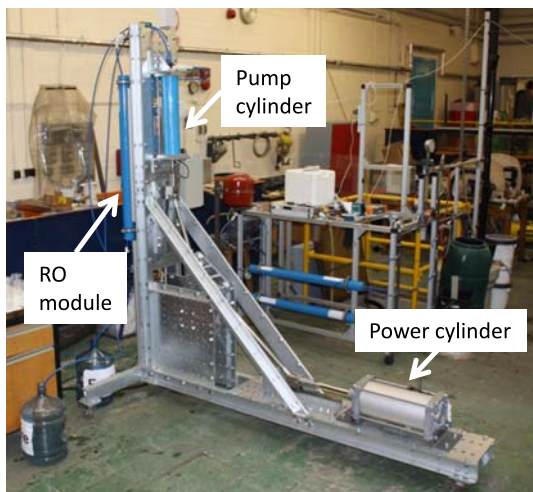


Fig. 10. Prototype of DesaLink.

DesaLink are the power cylinder, pump cylinder and RO module (see Fig. 10). The technical details of the two cylinders and the RO membrane module are presented in Table 1. NaCl solution of 4,000 ppm was used as feed water. To simulate steam, 8.8 barg compressed air was provided to the power cylinder to start the pressurisation phase, as depicted in Fig. 3. After several cycles, measurements were taken and the results are summarised in Table 2.

To investigate the performance of DesaLink under the conditions of steam generated by a solar collector, we assume the steam is superheated at 200°C and provides 10 bar pressure. Thus, for one cycle, 1.91 of steam (i.e. 0.01 kg) are required to produce 2.4 kg of permeate, which implies a gain output ratio of 240. To generate 0.01 kg of steam (without vacuum condenser system), it requires 24 kJ of heat; in another word, 90 W of heat input is needed to produce 321/h (based on 4.5 min of cycle time). For a simple type of solar collector with an efficiency of 35%, e.g. LFR, under solar radiation of 4 kWh/m² per day, requires only 0.5 m² of land area to produce 2561 of fresh water per 8 h a day. Note that these results are preliminary and it is expected to achieve improvements in speed and efficiency through further study and optimisation.

Table 2
Results of DesaLink prototype

Preliminary results			
Cycle duration	4 min	Permeate salinity	320 ppm
	30s		
Permeate per cycle	2.41	Brine salinity	11,000 ppm
Brine per cycle	11	Recovery ratio	70%

5. Conclusion

In the coming decades, undoubtedly, the demand for fresh water in inland area will increase, because of surging population growth and industrialisation. Advances in desalination system design can eliminate the energy conversion steps, thereby improving energy efficiency and reducing capital cost. This study has presented a batch process for desalination which is advantageous to achieve high recovery and high efficiency. The process has been demonstrated in principle using a materials testing (Instron[®]) machine. Further, a study of longitudinal dispersion has shown that this phenomenon is likely to deteriorate efficiency by only about 5%. Concentration polarisation has been studied systematically by use of Sherwood correlations to represent the mass transfer coefficient, which was found to be in the range $k = 3 \times 10^{-6} - 1.2 \times 10^{-5}$ m/s. The prototype DesaLink system operated reliably during the preliminary experimental tests under laboratory conditions using compressed air to simulate solar steam. It is predicted to achieve an output of 500 l/day per m² of solar collector. Future work will focus on optimisation of the system and trials under field conditions.

References

- [1] T.Y. Qiu, P.A. Davies, The scope to improve the efficiency of solar-powered reverse osmosis, *Desalin. Water Treat.* 35(1–3) (2011) 14–32.
- [2] S. Khan, D. Murchland, M. Rhodes, T.D. Waite, Management of concentrated waste streams from high-pressure membrane water treatment systems, *Crit. Rev. Environ. Sci. Technol.* 39(5) (2009) 367–415.
- [3] T. Younos, Environmental issues of desalination, *J. Contemp. Water Res. Edu.* 132(1) (2005) 11–18.
- [4] P.A. Davies, A solar-powered reverse osmosis system for high recovery of freshwater from saline groundwater, *Desalination* 271 (2011) 72–79.
- [5] M. Elimelech, W.A. Phillip, The future of seawater desalination: Energy, technology, and the environment, *Science* 333 (6043) (2011) 712–717.
- [6] T. Bowman, A. El-Nashar, B. Thrasher, A. Hussein, A. Unione, Design of a small solar-powered desalination system, *Desalination* 39 (1981) 71–81.
- [7] A.S. Nafey, M.A. Sharaf, Combined solar organic Rankine cycle with reverse osmosis desalination process: Energy, exergy, and cost evaluations, *Renew. Energy* 35(11) (2010) 2571–2580.
- [8] J. Bruno, J. López-Villada, E. Letelier, S. Romera, A. Coronas, Modelling and optimisation of solar organic Rankine cycle engines for reverse osmosis desalination, *Appl. Thermal Eng.* 28(17–18) (2008) 2212–2226.
- [9] J.J. Libert, A. Maurel, Desalination and renewable energies—a few recent developments, *Desalination* 39 (1981) 363–372.
- [10] D. Manolakos, G. Kosmadakis, S. Kyritsis, G. Papadakis, On site experimental evaluation of a low-temperature solar organic Rankine cycle system for RO desalination, *Solar Energy* 83(5) (2009) 646–656.
- [11] R.F. SERVICE, Desalination freshens up, *Science* (Washington, DC), 313(5790) (2006) 1088–1090.
- [12] T.Y. Qiu, P.A. Davies, Longitudinal dispersion in spiral wound RO modules and its effect on the performance of batch mode RO operations, *Desalination* 288 (2012) 1–7.

- [13] U. Merten, Flow relationships in reverse osmosis, *Ind. Eng. Chem. Fundament.* 2(3) (1963) 229–232.
- [14] P.L.T. Brian, Concentration polarization in reverse osmosis desalination with variable flux and incomplete salt rejection, *Ind. Eng. Chem. Fundament.* 4(4) (1965) 439–445.
- [15] L. Malaeb, G.M. Ayoub, Reverse osmosis technology for water treatment: State of the art review, *Desalination* 267(1) (2011) 1–8.
- [16] S. Sablani, M. Goosen, R. Al-Belushi, M. Wilf, Concentration polarization in ultrafiltration and reverse osmosis: A critical review, *Desalination* 141(3) (2001) 269–289.
- [17] E. Matthiasson, B. Sivik, Concentration polarization and fouling, *Desalination* 35 (1980) 59–103.
- [18] V. Gekas, B. Hallström, Mass transfer in the membrane concentration polarization layer under turbulent cross flow: I. Critical literature review and adaptation of existing Sherwood correlations to membrane operations, *J. Membr. Sci.* 30(2) (1987) 153–170.
- [19] M.S.H. Bader, J.N. Veenstra, Analysis of concentration polarization phenomenon in ultrafiltration under turbulent flow conditions, *J. Membr. Sci.* 114(2) (1996) 139–148.
- [20] DOW. DOW FILMTEC™ Membranes Production Information, Form No. 609-00350-0408.
- [21] G. Belfort, *Synthetic membrane processes: Fundamentals and water applications*, Academic Press, 1984.